

This article was downloaded by:[Bochkarev, N.]
On: 19 December 2007
Access Details: [subscription number 788631019]
Publisher: Taylor & Francis
Informa Ltd Registered in England and Wales Registered Number: 1072954
Registered office: Mortimer House, 37-41 Mortimer Street, London W1T 3JH, UK



Astronomical & Astrophysical Transactions

The Journal of the Eurasian Astronomical Society

Publication details, including instructions for authors and subscription information:
<http://www.informaworld.com/smpp/title~content=t713453505>

The time interferometer: A new tool for the spectral analysis of time series

V. V. Vityazev ^a

^a Astronomy Department, St.-Petersburg University, St.-Petersburg, Russia

Online Publication Date: 01 January 1994

To cite this Article: Vityazev, V. V. (1994) 'The time interferometer: A new tool for the spectral analysis of time series', *Astronomical & Astrophysical Transactions*, 5:1, 177

- 210

To link to this article: DOI: 10.1080/10556799408245872

URL: <http://dx.doi.org/10.1080/10556799408245872>

PLEASE SCROLL DOWN FOR ARTICLE

Full terms and conditions of use: <http://www.informaworld.com/terms-and-conditions-of-access.pdf>

This article maybe used for research, teaching and private study purposes. Any substantial or systematic reproduction, re-distribution, re-selling, loan or sub-licensing, systematic supply or distribution in any form to anyone is expressly forbidden.

The publisher does not give any warranty express or implied or make any representation that the contents will be complete or accurate or up to date. The accuracy of any instructions, formulae and drug doses should be independently verified with primary sources. The publisher shall not be liable for any loss, actions, claims, proceedings, demand or costs or damages whatsoever or howsoever caused arising directly or indirectly in connection with or arising out of the use of this material.

THE TIME INTERFEROMETER: A NEW TOOL FOR THE SPECTRAL ANALYSIS OF TIME SERIES

V. V. VITYAZEV

*Astronomy Department, St.-Petersburg University,
198904 St.-Petersburg, Petrodvorets, Bibliotechnaya pl. 2, Russia*

(Received January 27, 1993)

Gaps in observational time series due to factors beyond our control are habitually considered as a nuisance, since they make the spectral analysis of the time series much more complicated as compared with the case of regular observations. Nonetheless, in some applications the gaps may be found useful. It is shown that the spectral analysis of a multi-harmonic function given at two intervals, separated by a gap, yields the results very much similar to those which one has in the case of two antennas connected as an interferometer. This analogy leads to a conception of the Time Interferometer, which in some cases is superior to regular observations since it (a) makes the spectral lines sharper, (b) separates two close harmonics at the cost of sufficient reductions of time and observational expenditures, (c) improves the low frequency problem. This paper presents a theoretical foundation of the Time Interferometer and its application to astrometric time series.

KEY WORDS Time series, power spectra

1 INTRODUCTION

The "classical" spectral analysis of time series (Jenkins and Watts, 1968; Otnes and Enochson, 1978; Marple, 1987, et.) presumes that the observed data are represented either by continuous functions, or by samples with an even distribution in time. In astronomy, it is rather a rule that the time series are given at unequally spaced time points due to various factors – weather conditions, radiation belts, breakdowns, etc. To use the standard techniques of spectral evaluating, one needs such observations to be regularly spaced in time. Many approximate methods are used to do this preliminary step: interpolation, mean square fitting to a given function, averaging over a fixed interval, etc. While these methods may be satisfactory in some cases, they do not solve the problem in general.

The first rigorous analysis of unequally spaced data was performed perhaps by Deeming (1975). He showed that the periodograms of unevenly distributed data are contaminated by spurious details and explained how the "ghosts" may be recognized. In its modern state, the problem of gaps in observations may be described as

follows. We know nothing about the spectrum and gaps are beyond our control, so we are doing our best to extract, from the observed values, as much information as we could if the observations were regular. Several techniques (Delache and Scherer, 1983; Duvall and Harvey, 1984; Roberts *et al.*, 1987) encourage that the true spectrum may be reconstructed almost completely. In this connections one may ask whether it is always necessary to have regular observations, or in some applications it is possible to make observations with arranged gaps. This paper, presenting a rigorous study of the spectral analysis of data gathered in blocks and separated by gaps, gives a positive answer to this question.

2 THE SPECTRUM OF A MULTI-HARMONIC FUNCTION

We start by considering some theoretical aspects concerning the spectral analysis of deterministic functions given at arbitrary set of time points.

Suppose a time series is a multi-harmonic function,

$$x(t) = \sum_{k=1}^n A_k \cos(\omega_k t + \phi_k), \quad (2.1)$$

with amplitudes A_k , frequencies ω_k and phases ϕ_k of the harmonics. The corresponding auto-correlation function $k(\tau)$ and the true power spectrum $G(\omega)$ are

$$\begin{aligned} k(\tau) &= \lim_{T \rightarrow \infty} \frac{1}{T} \int_0^T x(t)x(t+\tau) dt \\ &= \frac{1}{2} \sum_{k=1}^n A_k^2 \cos(\omega_k \tau), \end{aligned} \quad (2.2)$$

$$\begin{aligned} G(\omega) &= \frac{1}{2\pi} \int_{-\infty}^{+\infty} k(\tau) \exp(-i\omega\tau) d\tau \\ &= \frac{1}{4} \sum_{k=1}^n A_k^2 [\delta(\omega - \omega_k) + \delta(\omega + \omega_k)], \end{aligned} \quad (2.3)$$

where $\delta = \delta(\omega)$ is Dirac's delta function. To describe the gaps in the observations, we introduce the *time window* function,

$$h(t) = \begin{cases} 1 & \text{if at time } t \text{ the data exists,} \\ 0 & \text{if at time } t \text{ the data is absent.} \end{cases} \quad (2.4)$$

With this notation, the observed time series may be represented as

$$y(t) = h(t)x(t). \quad (2.5)$$

It can be easily shown that the periodogram

$$D(\omega) = \frac{1}{2\pi T} \left| \int_0^T y(t) \exp(-i\omega t) dt \right|^2, \quad (2.6)$$

and the true spectrum $G(\omega)$ are related by

$$D(\omega) = \int_{-\infty}^{+\infty} G(\omega') H(\omega - \omega') d\omega' + D_0(\omega), \quad (2.7)$$

where

$$\begin{aligned} 4D_0(\omega) = & \sum_{p=1}^n A_p^2 [\Omega(\omega - \omega_p) \Omega^*(\omega + \omega_p) \exp(i2\phi_p) \\ & + \Omega^*(\omega - \omega_p) \Omega(\omega + \omega_p) \exp(-i2\phi_p)] \\ & + \sum_{\substack{p,q=1 \\ p \neq q}}^n A_p A_q [\Omega(\omega - \omega_p) \Omega^*(\omega + \omega_q) \exp(i(\phi_p + \phi_q)) \\ & + \Omega^*(\omega - \omega_p) \Omega(\omega + \omega_q) \exp(-i(\phi_p + \phi_q))] \\ & + \sum_{\substack{p,q=1 \\ p \neq q}}^n A_p A_q [\Omega(\omega - \omega_p) \Omega^*(\omega - \omega_q) \exp(i(\phi_p - \phi_q)) \\ & + \Omega(\omega + \omega_p) \Omega^*(\omega + \omega_q) \exp(-i(\phi_p - \phi_q))]. \end{aligned} \quad (2.8)$$

The functions Ω and H in Eqs. (2.7) and (2.8) are defined as follows:

$$\Omega(\omega) = \left[\frac{1}{2\pi T} \right]^{1/2} \int_0^T h(t) \exp(-i\omega t) dt, \quad (2.9)$$

$$H(\omega) = \Omega(\omega) \Omega^*(\omega) = \frac{1}{2\pi T} \left| \int_0^T h(t) \exp(-i\omega t) dt \right|^2. \quad (2.10)$$

Henceforth, the function $H(\omega)$ will be referred to as the *spectral window*.

Comments

1. A set of multi-harmonic functions (2.1) with the phases ϕ_k randomly distributed within the interval $[0, 2\pi]$ may be regarded as a stationary stochastic process. Averaging Eq. (2.8) over the set of realizations yields $E[D_0] = 0$, thus reducing Eq. (2.7) to a convolution of the true spectrum $G(\omega)$ with the spectral window $H(\omega)$. This result was obtained by Deeming (1975), who studied the periodogram averaged over a set of realizations, given at one and the same set of time points.

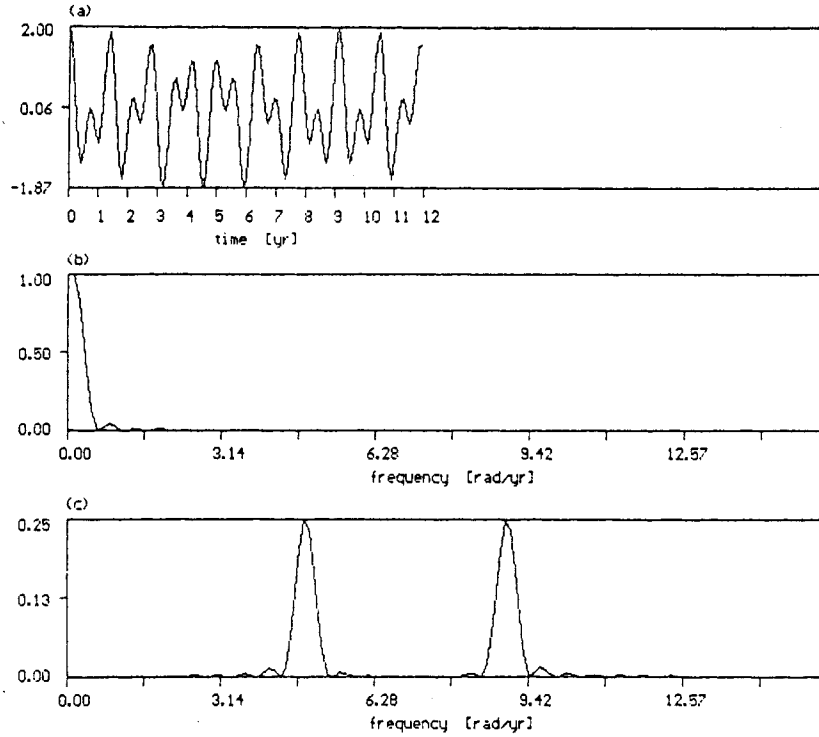


Figure 1 The spectral analysis of two cosinusoids with equal amplitudes, zero phases and the periods $P_1 = 1.3$ and $P_2 = 0.7$ yr: *a*, regular observations sampled at 120 points over 0.1 yr; *b*, the spectral window; *c*, the resulting spectrum.

2. If only one realization is available, there is nothing to average. In this case the term D_0 in Eq. (2.7) cannot be neglected. However, it can be shown that except for some highly specific, so to say, "pathological" cases, this term is small as compared with the convolution integral in Eq. (2.7).
3. Eqs. (2.6) and (2.7) are the basic tools in evaluating the observational spectrum $D(\omega)$ and in revealing the artifacts introduced by the missing data. Suppose the spectrum $G(\omega)$ has sharp features at $\omega = \pm\omega_0$,

$$G(\omega) = A[\delta(\omega - \omega_0) + \delta(\omega + \omega_0)], \quad (2.11)$$

where $A = \text{const.}$ According to Eq. (2.7), we obtain

$$D(\omega) = A[H(\omega - \omega_0) + H(\omega + \omega_0)] + D_0(\omega). \quad (2.12)$$

Hence, Eq. (2.12) describes the transformation of the initial spectrum $G(\omega)$ to the observed one $D(\omega)$. It is important to underline that the transformation from $G(\omega)$ to $D(\omega)$ is completely determined by the spectral window. If the data are irregularly spaced, the spectral window $H(\omega)$ usually has a central

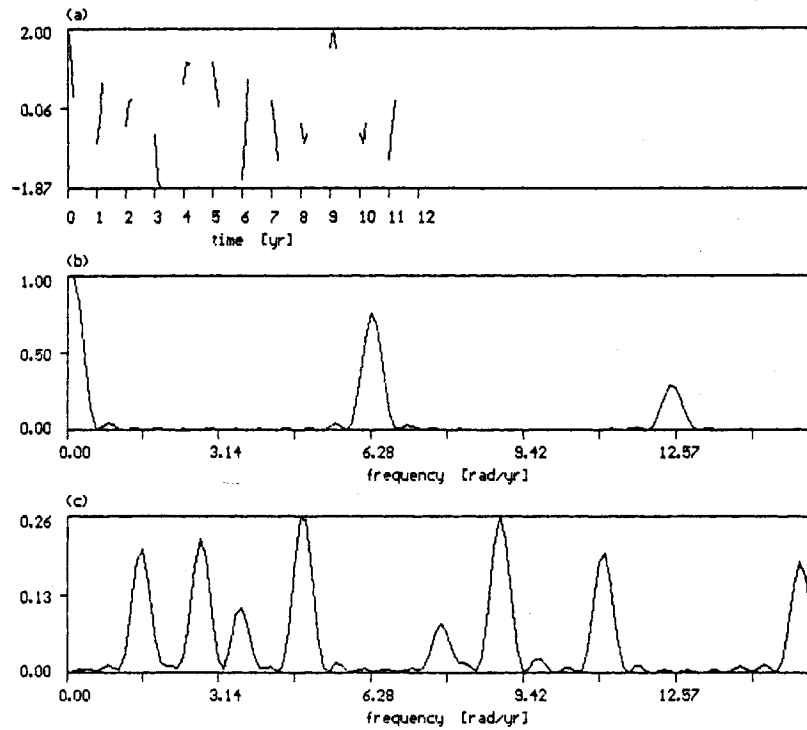


Figure 2 The same as in Figure 1: *a*, observations with 1 yr periodic gaps; *b*, the spectral window: the sidepeaks are centered at frequencies 2π and 4π rd/yr; *c*, a dirty spectrum: the highest peaks are real, all the rest are "ghosts".

peak at $\omega = 0$, the *sidepeaks* centered at some frequencies $\omega = \bar{\omega}_k$, $k = 1, 2, \dots$, and the *sidelobes* of the central peak and of the sidepeaks (Figure 2b). The sidelobes are caused by a finite time span of observations. They exist even for equally spaced data. The sidepeaks appear only if the data are spaced irregularly. According to Eq. (2.12) all these features are present in the observed spectrum. Indeed, the central peak is visible at $\omega = \omega_0$, and, showing the true features of the initial spectrum, it may be called the true peak. The sidepeaks are responsible for the spectral features at $\omega = |\omega_0 \pm \omega_k|$. The initial spectrum $G(\omega)$ has no lines at these frequencies. Hence, these features are false and may be regarded as "ghosts". To illustrate the results of the spectral analysis of evenly and unevenly distributed data, we consider two cosinusoids with periods $P_1 = 1.3$ yr, $P_2 = 0.7$ yr, sampled at 120 points over 0.1 yr regularly (Figure 1) and with annual gaps (Figure 2).

These are the only essential features which may be extracted from Eq. (2.7) in general case. If we need more, we are to have additional knowledge of the specific properties of the spectral windows.

3 ANALYTICAL STUDY OF SPECTRAL WINDOW FUNCTIONS

The standard way to study the spectral windows implies calculating $H(\omega)$ for a given set of time points. This calculation is performed each time when we do the spectral analysis. Unfortunately, it allows us to see the details in the spectral window, but not to explain them. To remedy this, we propose another approach. Its main idea lays in representing by regular observations with missing points of the situations frequently met in practice. Considered in this section are two examples: data spaced with periodic gaps and two sets of observations separated by a single gap. Both the cases, being of interest from practical point of view, lead us to quite a new understanding of unevenly spaced data, namely to the idea of the Time Interferometer.

3.1 Observations with Periodic Gaps

In real astronomical observations, gaps are either periodic or quasi-periodic. Ground-based observations are interrupted by meteorological changes, which, for a given site, are repeated annually. Night observations are stopped in the daytime, and such gaps follow with a 24-hour period. In both examples we have a certain cycle of observations, one part of which is filled with data, and the other is empty. To describe such situations, we introduce the following notation:

$\Delta t = \text{const}$	- the interval of sampling,
$\Delta T = (n + p)\Delta t$	- duration of one cycle of observations,
n	- number of observations in the cycle,
p	- number of missing points in the cycle,
m	- number of cycles,
$M = (n + p)m - p$	- total number of points in the time series,
$N = nm$	- total number of observations in the time series.

The sequence of cycles and the distribution of observations and gaps inside each cycle are shown in Figure 3.

Consider now two time window functions,

$$h_n(t) = \sum_{j=1}^n \delta[t - (j-1)\Delta t], \quad (3.1)$$

$$h_m(t) = \sum_{k=1}^m \delta[t - (k-1)\Delta T]. \quad (3.2)$$

The first one samples the observations within a cycle, the second one describes the sampling of cycles. Obviously, the resulting time window function is the convolution

$$h(t) = \int_{-\infty}^{+\infty} h_n(t') h_m(t-t') dt'. \quad (3.3)$$

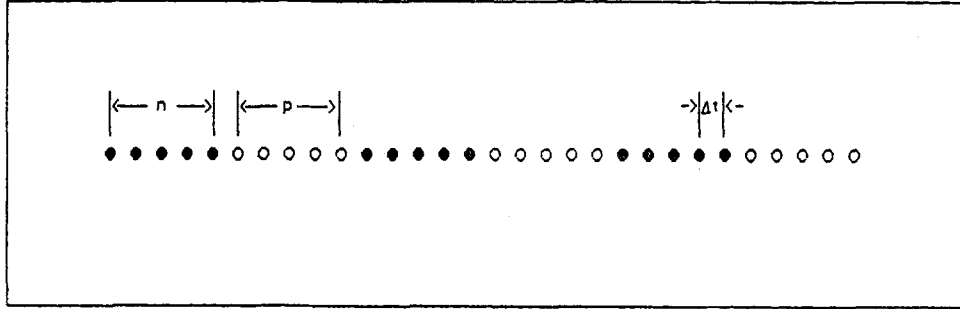


Figure 3 Observations with periodic gaps.

We are looking for the spectral window function

$$H(\omega) = \frac{1}{N^2} \left| \int_{-\infty}^{+\infty} h(t) \exp(-i\omega t) dt \right|^2, \quad (3.4)$$

satisfying the condition $H(0) = 1$. Using the theorem on the Fourier transform of a convolution, we get

$$H(\omega) = |\Omega_n(\omega)|^2 |\Omega_m(\omega)|^2, \quad (3.5)$$

where

$$\begin{aligned} \Omega_n &= \frac{1}{n} \int_{-\infty}^{+\infty} h_n(t) \exp(-i\omega t) dt \\ &= \frac{\sin(n\omega\Delta t/2)}{n \sin(\omega\Delta t/2)} \exp(-i\omega(n-1)\Delta t/2), \end{aligned} \quad (3.6)$$

$$\begin{aligned} \Omega_m(\omega) &= \frac{1}{m} \int_{-\infty}^{+\infty} h_m(t) \exp(-i\omega t) dt \\ &= \frac{\sin(m\omega\Delta T/2)}{m \sin(\omega\Delta T/2)} \exp(-i\omega(m-1)\Delta T/2). \end{aligned} \quad (3.7)$$

If we introduce the standard function,

$$H_0(\omega, N, \Delta t) = \frac{\sin^2(N\omega\Delta t/2)}{N^2 \sin^2(\omega\Delta t/2)}, \quad (3.8)$$

then for the spectral window under consideration we find

$$H(\omega) = H_0(\omega, n, \Delta t) H_0(\omega, m, \Delta T). \quad (3.9)$$

Thus we expressed the spectral window function of periodically interrupted observations in terms of the standard window function $H_0(\omega, N, \Delta t)$, corresponding to a

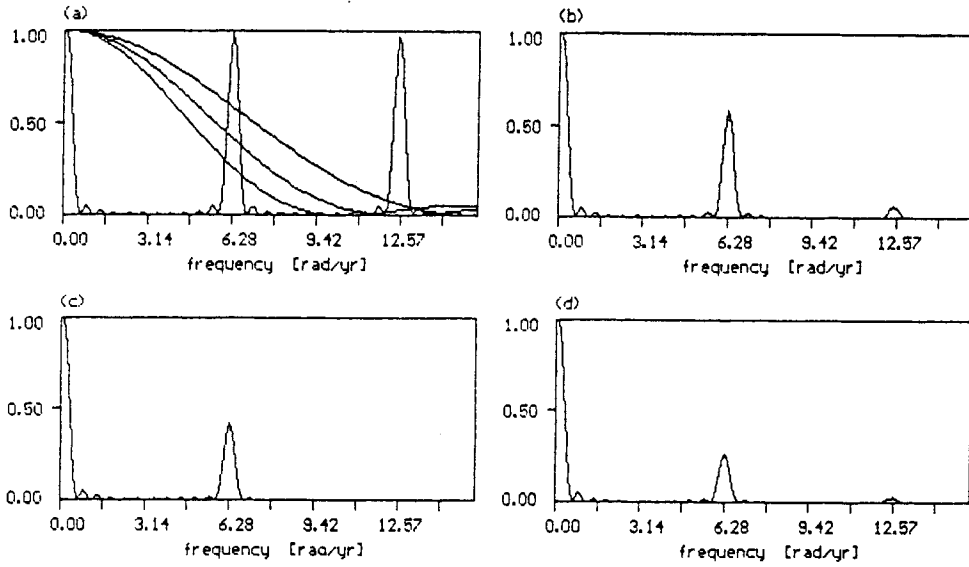


Figure 4 Spectral windows corresponding to observations with periodic gaps: *a*, standard windows $H_0(\omega, m = 12, \Delta T = 1)$; $H_0(\omega, n = 4, 5, 6; \Delta t = 0.1)$; *b*, $H(\omega, n = 4, \Delta t = 0.1)$; *c*, $H(\omega, n = 5, \Delta t = 0.1)$; *d*, $H(\omega, n = 6, \Delta t = 0.1)$.

set of N points equally spaced in time with an interval $\Delta t = \text{const}$. The function $H_0(\omega)$ is an even periodic function:

$$H_0(\omega, N, \Delta t) = H_0(-\omega, N, \Delta t), \quad (3.10)$$

$$H_0(\omega + 2n\omega_c, N, \Delta t) = H_0(\omega, N, \Delta t), \quad n = \pm 1, \pm 2, \dots, \quad (3.11)$$

where ω_c is the Nyquist frequency,

$$\omega_c = \pi/\Delta t. \quad (3.12)$$

The zeros of $H_0(\omega)$ are located at the frequencies

$$\omega_k = 2\pi k/N\Delta t, \quad k = \pm 1, \pm 2, \dots \quad (3.13)$$

It is instructive to illustrate the formation of the spectral window $H(\omega)$ as given by Eq. (3.9). Figure 4(a) shows narrow peaks and sidelobes of $H_0(\omega, m = 12, \Delta T = 1)$ running with the period $2\pi/\Delta T$ and broad central peaks of $H_0(\omega, n = 4; 5; 6, \Delta t = 0.1)$ on the interval $[0, \omega_c/2]$. Multiplication of these functions yields the results shown in Figure 4(b-d). The corresponding function $H(\omega)$ has central peaks and sidepeaks of decreasing intensities accompanied by a fine structure of the sidelobes. The sidepeaks are centered at

$$\bar{\omega}_k = 2\pi k/\Delta T, \quad k = \pm 1, \pm 2, \dots, (n + p), \quad (3.14)$$

and their intensities are given by

$$I_k \approx H_0(\bar{\omega}_k, n, \Delta t). \quad (3.15)$$

The frequencies $\bar{\omega}_k$, defined by Eq. (3.14), are of special interest for us, and we shall call them the Proper Frequencies (PF). Correspondingly, we can introduce the Proper Periods (PP),

$$P_k = \frac{2\pi}{\bar{\omega}_k} = \frac{\Delta T}{k}, \quad k = 1, 2, \dots, (n + p). \quad (3.16)$$

Now we see that the first (and the largest) sidepeak displays the period of gaps, while the others form the sequence $\Delta T/2, \Delta T/3$, etc. Since the positions of the zeros of $H_0(\omega, n, \Delta t)$ depend on the number of observations within ΔT , some of the sidepeaks may be suppressed. Figure 4(c) shows an example corresponding to $n = p$ (one half of ΔT is filled, the other is empty). Here only the first sidepeak appears, while the second one is absent, since it is located exactly at the zero of $H_0(\omega, n, \Delta t)$.

3.2 Two Observational Sets Separated by a Gap

Sometimes observations which lasted for a certain period are interrupted, and after a lapse of time they are resumed. As a result, we have two time series separated by a gap. To describe the situation, we use the following notation:

- n_1, n_2 - the numbers of equally spaced data in the first and second blocks of information,
- p - the number of missing points, forming the gap,
- $M = n_1 + n_2 + p$ - the total number of points in the whole time series,
- $N = n_1 + n_2$ - the total number of observed points.

The distribution of time points corresponding to the situation is shown in Figure 5. For the case under consideration, the time window function is given by

$$\begin{aligned} h(t) &= h_1(t) + h_2(t) \\ &= \sum_{k=1}^{n_1} \delta(t - k\Delta t) + \sum_{k=n+p+1}^M \delta(t - k\Delta t). \end{aligned} \quad (3.17)$$

Now, according to Eq. (3.4), the corresponding spectral window is

$$\begin{aligned} H(\omega) &= \frac{n_1^2}{(n_1 + n_2)^2} H_0(\omega, n_1, \Delta t) + \frac{n_2^2}{(n_1 + n_2)^2} H_0(\omega, n_2, \Delta t) \\ &+ \frac{2n_1 n_2}{(n_1 + n_2)^2} [H_0(\omega, n_1, \Delta t) H_0(\omega, n_2, \Delta t)]^{1/2} \cos(M + p)\omega\Delta t/2. \end{aligned} \quad (3.18)$$

From Eq. (3.18) it is clear that if each block of observations were treated separately, the corresponding spectral window would be either $H_0(\omega, n_1, \Delta t)$ or

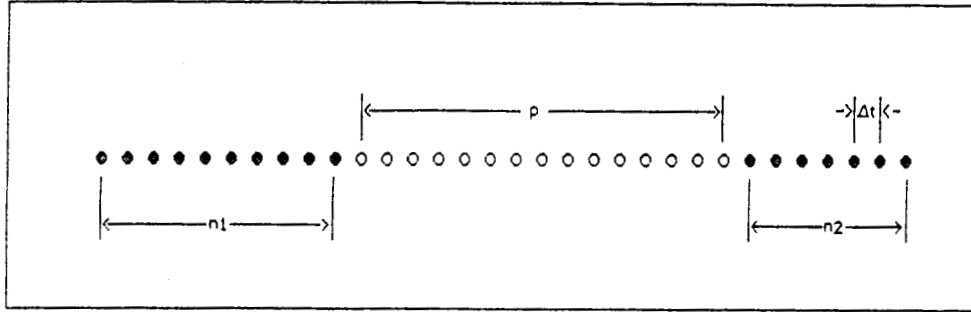


Figure 5 Observations with a gap.

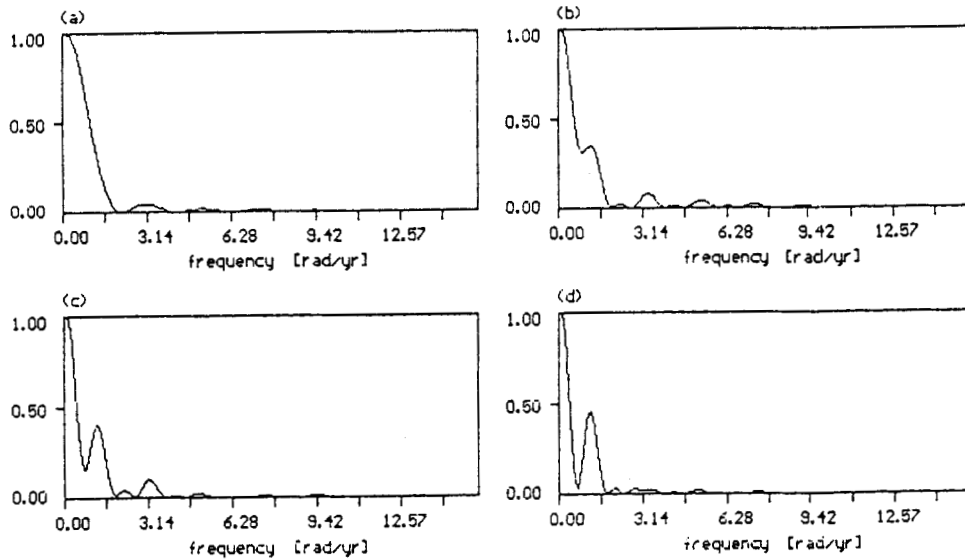


Figure 6 The spectral windows of two unequal blocks of observations: a, $n_1 = 30, p = 0, n_2 = 0$; b, $n_1 = 30, p = 30, n_2 = 5$; c, $n_1 = 30, p = 30, n_2 = 10$; d, $n_1 = 30, p = 30, n_2 = 20$.

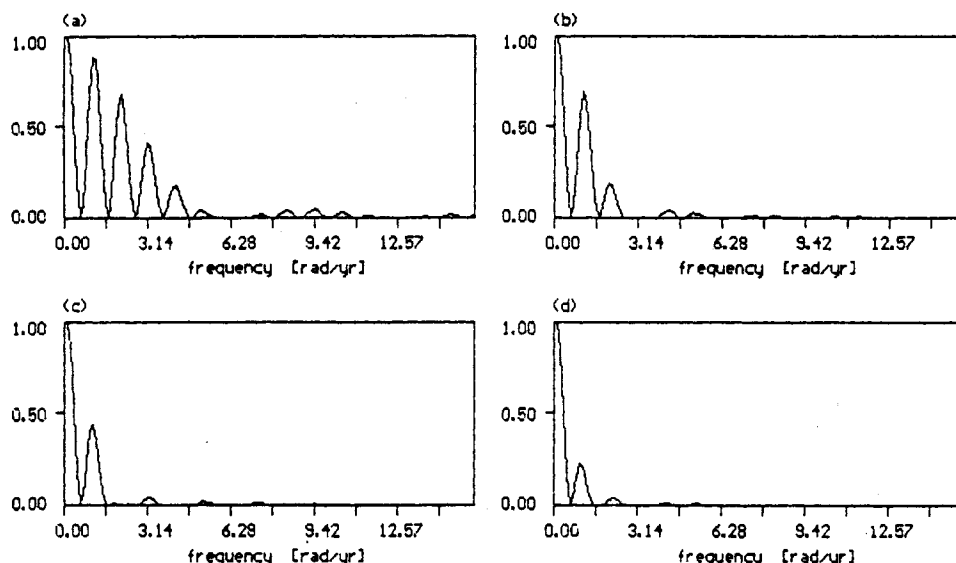


Figure 7 The spectral windows of two equal blocks of observations: a, $n_1 = 10, p = 50, n_2 = 10$; b, $n_1 = 20, p = 40, n_2 = 20$; c, $n_1 = 30, p = 30, n_2 = 30$; d, $n_1 = 40, p = 20, n_2 = 40$.

$H_0(\omega, n_2, \Delta t)$. Figure 6 shows how the function $H(\omega)$ changes when observations of the second block are added to the first block. As n_2 increases, the central peak of $H(\omega)$ changes its form, and at frequencies

$$\bar{\omega}_k = \frac{-4\pi k}{(M+p)\Delta t}, \quad k = 1, 2, \dots, \quad (3.19)$$

for which the cosine in Eq. (3.15) is unity, the embryos of the sidepeaks gradually develop.

Let us consider now the most interesting case of two equal series separated by a gap. For $n = n_1 = n_2$, Eq. (3.15) yields

$$H(\omega) = \frac{1 + \cos(n+p)\omega\Delta t}{2} H_0(\omega, n, \Delta t). \quad (3.20)$$

We would obtain the same expression if we had taken $m = 2$ in Eq. (3.9). Hence the structures of the spectral windows corresponding to periodic gaps and to a single gap are basically similar. In both cases the sidepeaks, located at PF,

$$\bar{\omega}_k = \frac{2\pi k}{(n+p)\Delta t}, \quad k = 1, 2, \dots \quad (3.21)$$

are present. Figure 7 illustrates the structure of spectral windows for the case of two equal blocks of observations, corresponding to three cases: the gap is wider ($p > n$), equal ($p = n$) and narrower ($p < n$) than each block of observations. We see that the longer is the gap, the higher are the sidepeaks.

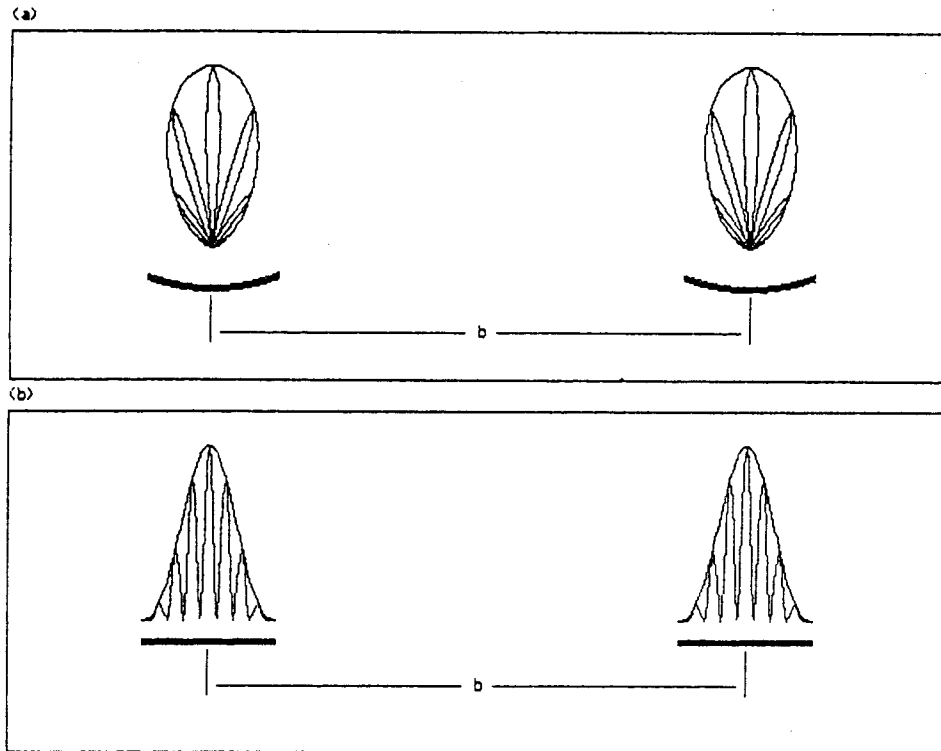


Figure 8 The analogy of interferometers: *a*, the space interferometer implies a separation of antennas in space and observations made at one and the same point (interval) of time; *b*, the Time Interferometer implies a separation of "antennas" in time and observations made at one and the same point (site) of space.

4 THE TIME INTERFEROMETER

Upon close examination, it turns out that if we treat each block of observations separately, we have a rather broad spectral window, whereas a combined treatment of the blocks results in splitting the central peak into several narrow sidepeaks. The situation is similar to what one has in an interferometer, for, as we know, the central beam of each telescope is splitted into several lobes if two telescopes are connected to form an interferometer. Figure 8 displays this remarkable analogy. There is a good reason to call sets of observations with gaps the *Time Interferometer*. Keeping in mind that results of experiments may be referred not to time but to any other variable, a more general term – the *Numerical Interferometer* would also be natural.

The quantity

$$b = \frac{M + p}{2} \Delta t = (n_1/2 + p + n_2/2) \Delta t \quad (4.1)$$

is essentially the *baseline* of the Time Interferometer. Now, the Proper Periods of one gap spectral window can be represented as

$$P_k = \frac{b}{k}, \quad k = 1, 2, \dots \quad (4.2)$$

So, the period of the first sidepeak reveals the length of the baseline. The same interpretation of the PP is implied by Eq. (3.16). Now, while a series of observations with a single gap corresponds to a simple two-element interferometer, a series of periodically interrupted observations corresponds to an array of equidistant antennas (a grating interferometer). Having established the correspondence between the space interferometer and the time interferometer, we find that the gaps in observational series stand for the spacings between the antennas. Our main general conclusion is as follows: the laws of interferometry govern many problems we meet in the spectral analysis of time series.

5 WHAT CAN THE TIME INTERFEROMETER DO?

In this section we discuss several typical situations, when gaps in observations are useful. For all the cases we consider, the results are specific to regular observations and to distributions of time points with gaps. Using the terminology of interferometry, we can introduce several types of "time telescopes":

- a) A Simple Antenna (SA), i.e. a time series given at N equidistant points over the interval $\Delta t = \text{const}$. The total time span $T = (N - 1)\Delta t$ is the numerical counterpart of the diameter of the antenna. The beam of the antenna is the spectral window function $H_0(\omega, N, \Delta t)$, defined by Eq. (3.8).
- b) A Simple Time Interferometer (STI), i.e. a set of two data blocks separated by a gap. The numbers of observations in the blocks are n_1 and n_2 , the gap consists of p points, all the points are equidistant with an interval $\Delta t = \text{const}$. The baseline of the STI is given by Eq. (4.1), and the length of the STI in time (duration) is $L = (n_1 + p + n_2 - 1)\Delta t$. The numerical counterpart of the interference fringe system is the spectral window function $H(\omega)$, defined by Eq. (3.18).
- c) A Grating Time Interferometer (GTI), i.e. a set of data blocks separated by gaps. Each block consists of n observations, each gap consists of p points. All the points are equidistant with an interval $\Delta t = \text{const}$. The main period of gaps is $\Delta T = (n + p)\Delta t$, the duration of the GTI is $L = [(n + p)m - p - 1]\Delta t$. The dirty beam of the GTI is described by the spectral window function (3.9).

5.1 The Frequency Resolution

In spectral analysis, the quality of a spectrum is estimated by its *frequency resolution*. This is the frequency band, within which spectral details are not separable

Table 1. Numerical values of χ in Eq. 5.3

n_2/n_1	p/n_1		
	0.5	1	2
0.05	0.573	0.393	-
0.10	0.642	0.502	-
0.20	0.750	0.668	0.609
0.25	0.788	0.722	0.677
0.30	0.819	0.764	0.727
0.40	0.865	0.823	0.760
0.50	0.894	0.861	0.840
0.60	0.914	0.886	0.867
0.70	0.926	0.901	0.885
0.80	0.934	0.911	0.895
0.90	0.939	0.917	0.901
1.00	0.941	0.919	0.903
1.50	0.939	0.911	0.889
2.00	0.931	0.894	0.861
3.00	0.920	0.870	0.815
4.00	0.918	0.860	0.789
5.00	0.920	0.859	0.778

The frequency resolution is measured by the width of spectral lines. In theory, when a multi-harmonic function is known for any time t , the spectral lines are given by delta functions. They are infinitesimally wide. In reality, the time span of observations is finite, and the delta functions are replaced by spectral window functions. The central peaks of the spectral windows have the profiles which depend on the distribution of the samples. For this reason, the comparison of the spectral windows is possible only with a certain measure which has one and the same meaning for each case. The commonly used measure of the width of the central peak is the half-power width. If this measure is adopted, then the frequency resolution of the SA can be evaluated as

$$q_N = \lambda_1 \frac{2\pi}{N\Delta t}, \quad (5.1)$$

where $\lambda_1 = 0.89$ for $N \geq 10$. In the case of the STI, the corresponding value can be represented in the form

$$q_b = \lambda_2 \frac{\pi}{b}, \quad (5.2)$$

where λ_2 depends on n_2/n_1 and p/n_1 . Equating q_N and q_b , we find

$$N\Delta t = \chi 2b, \quad (5.3)$$

where $\chi = \lambda_1/\lambda_2$. The numerical values of χ are shown in Table 1.

From Eq. (5.3) it follows that to achieve equal frequency resolution, using STI and SA, the durations of the experiment and the required number of observations

Table 2. Gain of duration, GD , per cent (STI as compared to SA)

n_2/n_1	p/n_1		
	0.5	1	2
0.05	-32	-71	-
0.10	-19	-35	-
0.20	-3	-3	-1
0.25	1	4	9
0.30	5	9	14
0.40	8	14	21
0.50	11	17	24
0.60	12	19	26
0.70	12	19	27
0.80	12	19	27
0.90	12	19	27
1.00	12	18	26
1.50	9	15	22
2.00	6	11	17
3.00	2	4	8
4.00	0	0	1
5.00	-1	-2	-3

are different. It is useful to introduce two numbers, DD and DO , to measure the relative efficiency of SA and STI in spectral resolution: the difference of durations

$$DD = T - L = [p(2\chi - 1) + (n_1 + n_2)(\chi - 1)]\Delta t, \quad (5.4)$$

and the difference of observations

$$DO = N - (n_1 + n_2) = \chi 2p + (n_1 + n_2)(\chi - 1). \quad (5.5)$$

From Eqs. (5.4) and (5.5) one can see that if χ is close to unity, then

$$DD \approx p\Delta t, \quad (5.6)$$

$$DO \approx 2p. \quad (5.7)$$

In other words, the difference of durations is approximately equal to the length of the gap, whereas the difference of observations is almost twice the number of missing points. The gains in time and labor expenditures $GD = DD/T$, $GO = DO/N$ are shown in Tables 2 and 3. It is instructive to analyze the Tables, assuming that the observations of the second block are added point by point to the first block. One can see that

- a) the two-element Time Interferometer becomes shorter than the corresponding Simple Antenna, starting from the value $n_2/n_1 \approx 0.25$ and remains to be shorter up to $n_2/n_1 \approx 4$;

Table 3. Gain of observations, GO , per cent (STI as compared to SA)

n_2/n_1	p/n_1		
	0.5	1	2
0.05	11	12	—
0.10	19	29	—
0.20	27	45	62
0.25	30	47	65
0.30	31	48	66
0.40	33	50	67
0.50	33	50	68
0.60	33	50	67
0.70	32	49	66
0.80	31	48	65
0.90	30	47	64
1.00	29	46	63
1.50	24	39	57
2.00	19	33	50
3.00	13	23	39
4.00	10	17	30
5.00	7	13	23

b) the Time Interferometer provides the same frequency resolution using less observations than the Simple Antenna needs.

The most favourable situation for both GD and GO takes place if

$$0.5 < \frac{n_2}{n_1} < 1 \quad (5.8)$$

for every fixed ratio p/n_1 . The gains grow up while this ratio increases for every fixed value of n_2/n_1 . Hence, the longer is the gap, the less expensive are the interferometric results as compared with the regular observations. The efficiency can be increased if we are able to organize the experiments in such a way that the spare time of the gap could be filled with observations of other programs.

Similarly, we may consider the GTI. In this case the half-width of the central peak is

$$q_m = \lambda_3 \frac{2\pi}{m\Delta T}, \quad (5.9)$$

where λ_3 depends on p/n and m . Equating q_N and q_m , we obtain

$$N\Delta T = \chi m\Delta T, \quad (5.10)$$

where $\chi = 0.89/\lambda_3$. The corresponding differences of durations and of the number of observations now are

$$DD = T - L = [p(1 + m(\chi - 1)) + mn(\chi - 1)]\Delta t, \quad (5.11)$$

$$DO = N - mn = \chi mp + mn(\chi - 1). \quad (5.12)$$

Table 4. Numerical values of χ in Eq. 5.10

m	$p/(n+p)$		
	0.7	0.5	0.3
2	0.895	0.914	0.941
4	0.975	0.979	0.986
6	0.989	0.991	0.994
8	0.994	0.995	0.997
10	0.996	0.997	0.998
50	1.000	1.000	1.000

Table 5. Gain of duration, GD , per cent (GTI as compared to SA)

m	$p/(n+p)$		
	0.7	0.5	0.3
2	27	18	10
4	15	11	6
6	11	8	4
8	8	6	3
10	7	5	3
50	1	1	1

Table 6. Gain of observations, GO , per cent (GTI as compared to SA)

m	$p/(n+p)$		
	0.7	0.5	0.3
2	66	45	26
4	69	49	29
6	70	50	30
8	70	50	30
10	70	50	30
50	70	50	30

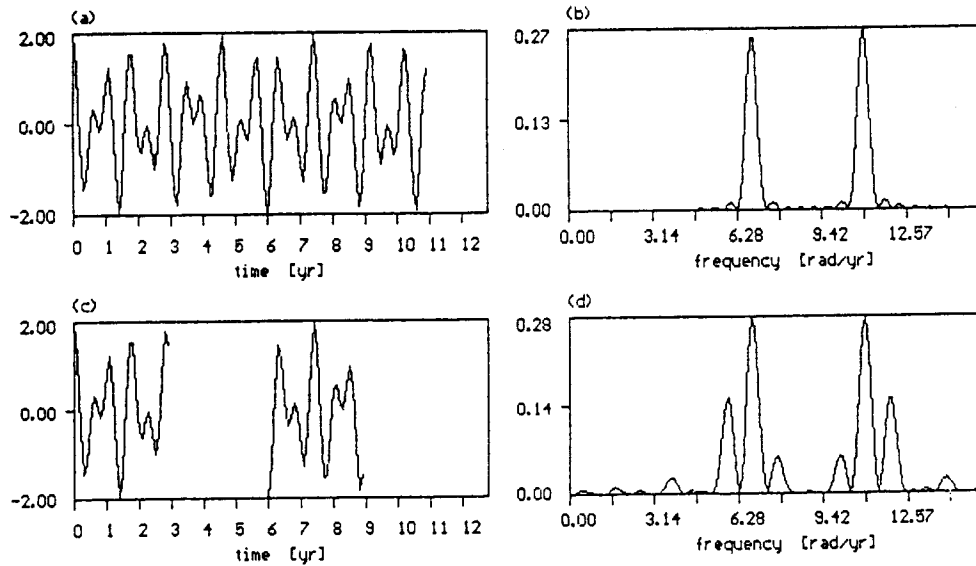


Figure 9 The spectral analysis of two cosine functions with periods $P_1 = 0.923$ and $P_2 = 0.571$ yr: a, regular observations consisting of 110 points, spaced by 0.1 yr; b, the resulting spectrum; c, the Time Interferometer ($n_1 = 30$, $p = 30$, $n_2 = 30$); d, the resulting spectrum.

The numerical values of χ and of the gains of time and labour expenditures GD and GO , corresponding to the GTI, are shown in Tables 4–6. From these Tables one can see that the GTI, consisting of a small number of two-element interferometers ($m \leq 6$), reduces the duration of the experiment by up to 4–27 per cent. As to the gains of observations, the GTI always yields the gains which are very well estimated by the ratio $p/(n+p)$.

5.2 The Sharpness of Spectral Lines

It is quite obvious that the narrower a spectral line is, the more accurate its central frequency may be evaluated. As it was pointed out, the frequency resolution and the half-power width of a spectral line are practically one and the same thing. For this reason, all the beneficial properties of the Time Interferometer concerning the frequency resolution may be applied to the sharpness of lines. Figures 9(a, b) show the spectrum of two cosine functions generated at 110 equidistant points without gaps, and Figures 9(c, d) show the spectrum of the same functions, but represented as the Time Interferometer with parameters $n_1 = n_2 = 30$, $p = 30$. We see that the lines in both spectra have equal half-power widths ($q = 0.51$ rd/yr), though the STI required for this purpose less time and less observations.

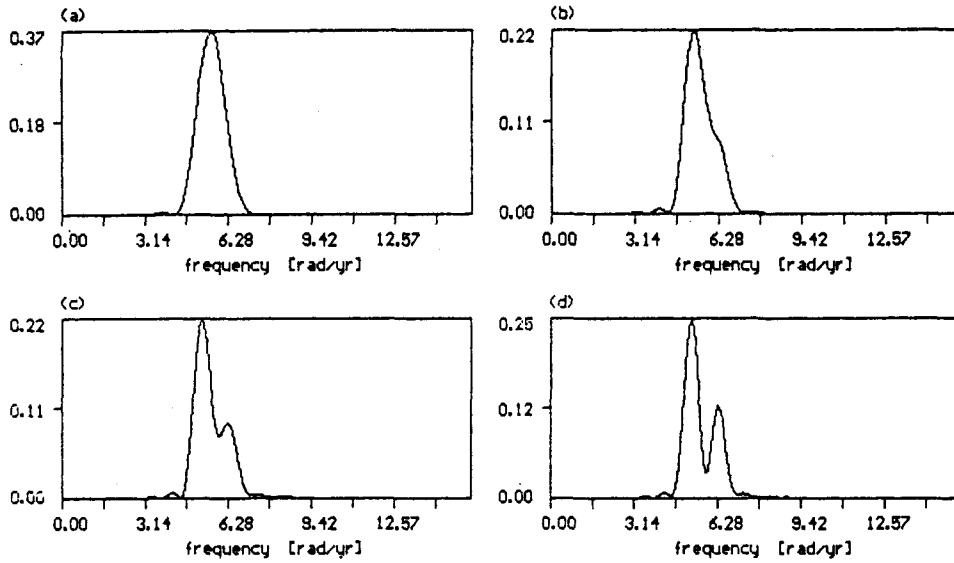


Figure 10 The separation of two cosinusoids: $A_1 = 0.7$, $P_1 = 1.0$ yr, $\phi_1 = 0$; $A_2 = 1$, $P_2 = 1.2$ yr and $\phi = \pi$: a, no separation is visible ($N_0 = 54$, $C = 0$); b, the separation appears ($N_0 = 75$, $C = 0$); c, a partial separation ($N_0 = 80$, $C = 0.10$); d, a partial separation ($N_0 = 90$, $C = 0.55$). A complete separation is shown in Figure 11(b).

5.3 Separation of Spectral Lines

The striking ability of space interferometer to discriminate between two close sources on the celestial sphere is a motivation to consider the same ability of the Time Interferometer. Two harmonics specified by frequencies ω_k , amplitudes A_k and phases ϕ_k , $k = 1, 2$ are said to be separated (resolved), if one can see in the spectrum two maxima placed at frequencies ω_1, ω_2 together with a minimum at $(\omega_1 + \omega_2)/2$. The separation may be measured by the *contrast*

$$C = \frac{I_{max} - I_{min}}{I_{max} + I_{min}}, \quad (5.13)$$

where I_{min} means the spectral power at the minimum, I_{max} the spectral power at the lower maximum. The contrast of separation depends on the total time span of the observations, on the frequencies and on the amplitudes of the harmonics. If $C = 1$, then the separation is complete, if $C < 1$, we have a partial separation. In the case when no minimum is visible, the lines are unresolved, and, setting $I_{min} = I_{max}$, we get $C = 0$.

In the case of regular observations, for every set of parameters ω_k, A_k, ϕ_k , $k = 1, 2$ two quantities may be introduced. One of them is N_0 , which is the upper limit of the total number of observations when the lines are not resolved ($C = 0$). The other is the number of observations N_1 , corresponding to a complete separation of the

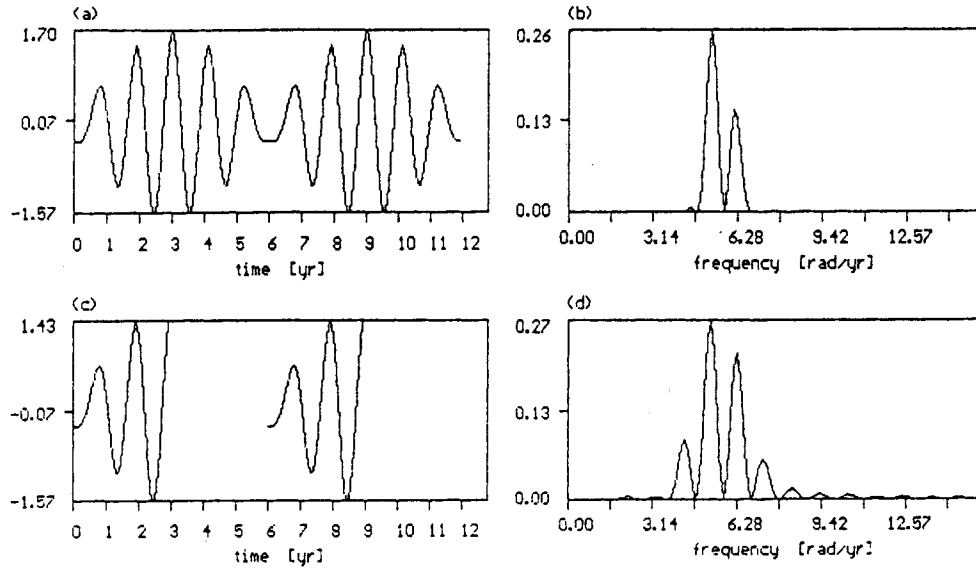


Figure 11 A complete separation of the same cosinusoids as in Figure 10: *a*, regular observations consisting of 120 points over interval 0.1 yr; *b*, the resulting spectrum; *c*, the Time Interferometer ($n_1 = 30$, $p = 30$ and $n_2 = 30$); *d*, the resulting spectrum. The Time Interferometer provides 25 per cent gain of time and 50 per cent gain of observations.

lines ($C = 1$). In all intermediate cases ($N_0 < N < N_1$) the separation is incomplete ($C < 1$). Figures 10 and 11(b) show a successive separation of two cosine functions with parameters

$$\begin{aligned} A_1 &= 0.7, & P_1 &= 1.0 \text{ yr}, & \phi_1 &= 0, \\ A_2 &= 1.0, & P_2 &= 1.2 \text{ yr}, & \phi_2 &= \pi, \end{aligned} \quad (5.14)$$

(the time series, composed of cosinusoids (5.14), will be used in the following subsections as a working model).

Consider now the case of complete separation. Two harmonics are said to be resolved completely if

$$|\omega_1 - \omega_2| = \Delta\omega, \quad (5.15)$$

where $\Delta\omega$ stands for the width of spectral lines, measured from one zero point to the other. For the SA, in accordance with Eq. (3.13), we may take

$$\Delta\omega = \frac{4\pi}{N_1 \Delta t}. \quad (5.16)$$

Thus, the total number of observations sufficient to resolve the harmonics completely is

$$N_1 = \frac{4\pi}{|\omega_1 - \omega_2| \Delta t}. \quad (5.17)$$

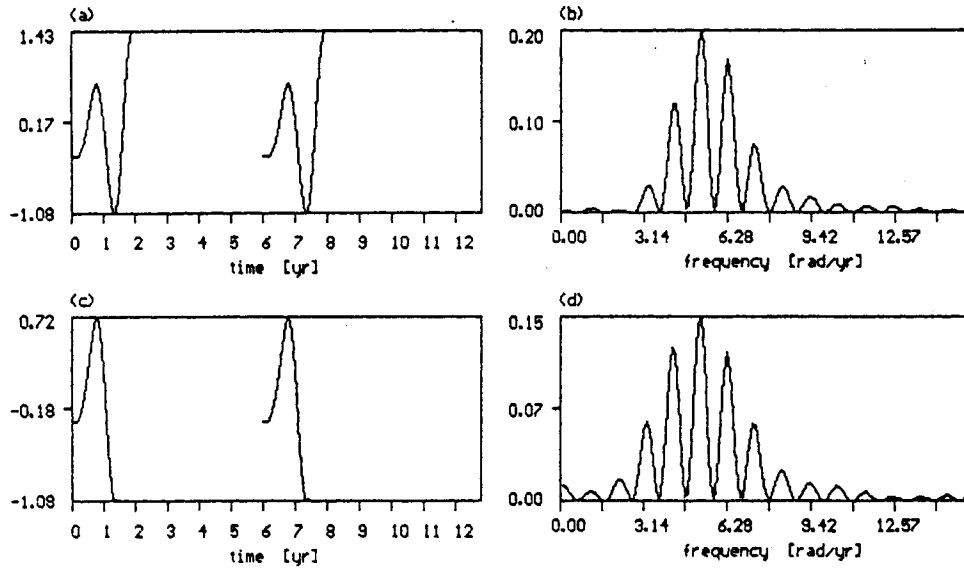


Figure 12 The same as in Figure 11: a, the Time Interferometer ($n_1 = 20, p = 40, n_2 = 20$); b, the resulting spectrum; c, the Time Interferometer ($n_1 = 15, p = 45, n_2 = 15$); d, the resulting spectrum. Comparison with regular observations (Figures 11(a), 11(b)) yields 33 and 37.5 per cent gains of time and 68 and 75 per cent gains of observations, correspondingly.

In the case of the equal block STI, we may replace Eq. (5.11) by

$$\Delta\omega = \frac{2\pi}{b}, \tag{5.18}$$

which for the baseline of the STI yields

$$b = \frac{2\pi}{|\omega_1 - \omega_2|}. \tag{5.19}$$

The comparison of Eqs. (5.16) and (5.18) yields again Eq. (5.3) but now with $\chi = 1$. This means that, with respect to a complete resolution of the two harmonics, the STI with the baseline b is preferable to the SA with the "aperture" $N_1 \Delta t = b$ since the STI resolves close lines faster than the SA, and requires less observations to be made. The gain of time and labour expenditure may be estimated with the help of Eqs. (5.4) and (5.5) (with $\chi = 1$). It is also remarkable that the resolution condition (5.19) defines only the length of the baseline and leaves free n and p . In other words, to separate the harmonics with frequencies ω_1 and ω_2 , one may construct a multitude of equal block interferometers with various values n and p , provided that the sum $n+p$ remains unchanged. Figures 11, 12 demonstrate various ways of observations needed to resolve the same functions as in Figure 10, as well as the estimates of the profit we gain replacing regular observations by the equal block Time Interferometer.

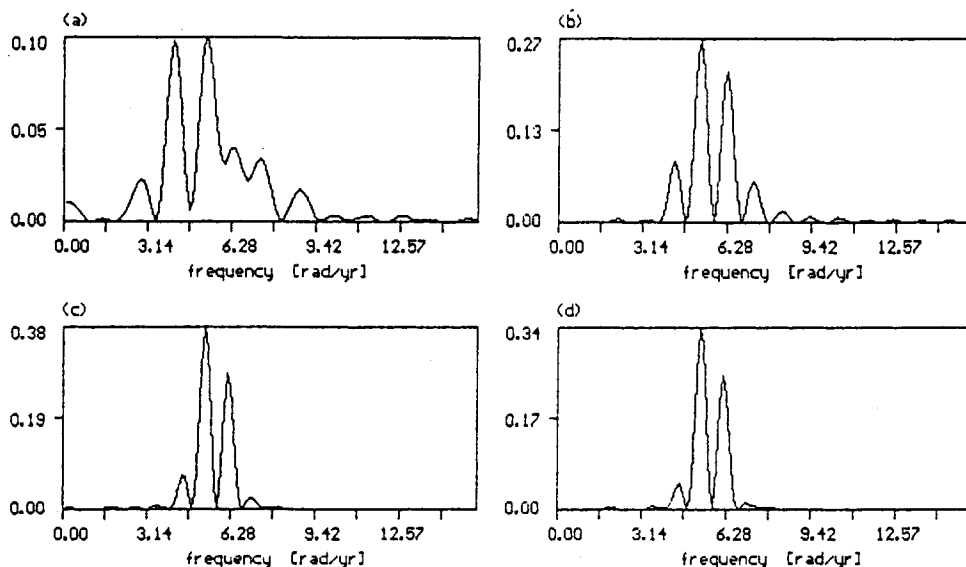


Figure 13 Separation of the same sinusoids as in Figure 10, made by equal block Time Interferometers with variable baselines and variable amounts of observations: a, $n_1 = 20$, $p = 30$, $n_2 = 20$; $b = 5.0$ yr, $M = 70$, $C = 0.12$; b, $n_1 = 30$, $p = 30$, $n_2 = 30$; $b = 6.0$ yr, $M = 90$, $C = 1.00$; c, $n_1 = 40$, $p = 30$, $n_2 = 40$; $b = 7.0$ yr, $M = 110$, $C = 0.96$; d, $n_1 = 45$, $p = 30$, $n_2 = 45$; $b = 7.5$ yr, $M = 120$, $C = 0.97$.

In some applications (when discovery or confirmation of a double structure is needed), it is quite sufficient to have a partial separation of the lines. As we have seen, in the case of the SA the partial resolution of two lines takes place if the total amount of observations is less than the specific value defined by Eq. (5.17). When the Time Interferometer is used, a partial separation occurs under two circumstances. The first one is specific for the STI with equal blocks when condition (5.19) is not satisfied. Figure 13 shows the spectra of our sinusoids (5.14) following from the equal block STI, for which the baselines and the total numbers of observations are changing from $b = 5.0$ to 7.5 yr, and from $M = 70$ to 120 , respectively. These figures tell us that the STI may yield a good separation even if we know the periods *a priori* with an error of about 30 per cent. Another example of partial separation is the STI with unequal blocks of observations ($n_1 \neq n_2$). As we have seen in Sect. 3, if $n_2 < n_1/2$, then the first sidepeak of the spectral window is not separated completely from the central peak, while the upper part of the central peak becomes narrower as compared with its width corresponding to $n_2 = 0$. Figure 14 demonstrates the ability of the STI with unequal blocks to separate our sinusoids. The comparison of Figures 10(c), 13(a), 14(b) leads us to a very important conclusion: with respect to partial separation of spectral lines, the Time Interferometer is again preferable over the SA, since with $M = 70$ the STI produces the separation of our lines with such a value of the contrast ($C = 0.12 \div 0.19$), for which the SA

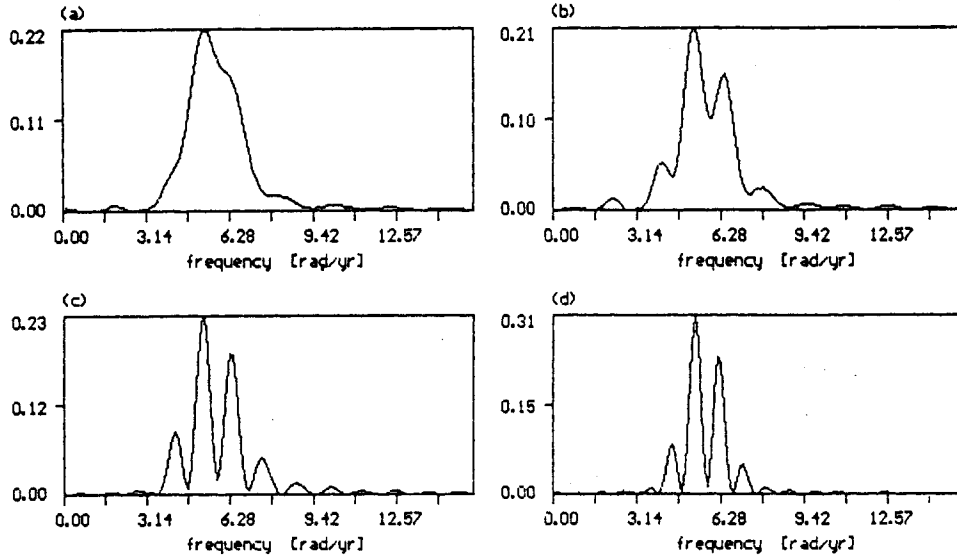


Figure 14 Separation of the same cosinusoids as in Figure 10, made by non-equal block Time Interferometers: a, $n_1 = 30$, $p = 30$, $n_2 = 5$; $b = 4.75$ yr, $M = 65$, $C = 0.00$; b, $n_1 = 30$, $p = 30$, $n_2 = 10$; $b = 5.0$ yr, $M = 70$, $C = 0.19$; c, $n_1 = 30$, $p = 30$, $n_2 = 20$; $b = 5.5$ yr, $M = 80$, $C = 0.80$; d, $n_1 = 30$, $p = 30$, $n_2 = 40$; $b = 6.5$ yr, $M = 100$, $C = 0.97$.

requires 80 observations. And still one remark is to be made. Figures 13(a) and 14(b) show that in the case of the equal block interferometer the sidepeaks are much more pronounced if compared with the non-equal block interferometer. From this point of view, the latter interferometer is preferable to the former, since it allows to suppress false details in the spectrum making it almost clean.

5.4 The Lowest Frequency Component

The resolution power of the Time Interferometer may be used for contribution to the so-called problem of low frequencies. In the case of equally spaced time points, the lowest frequency which may be recognized in a spectrum is the one which is separated from the zero-point by a distance equal to a half-width of the spectral window (measured from one zero point to another),

$$\omega_{min}^{(N)} = \frac{2\pi}{N\Delta t}. \quad (5.20)$$

In the case of the equal block STI we may take the half-width of a central peak to get

$$\omega_{min}^{(b)} = \frac{\pi}{b}. \quad (5.21)$$

These results being reformulated in terms of periods imply that the longest period, which can be established from a set of equally spaced data, is

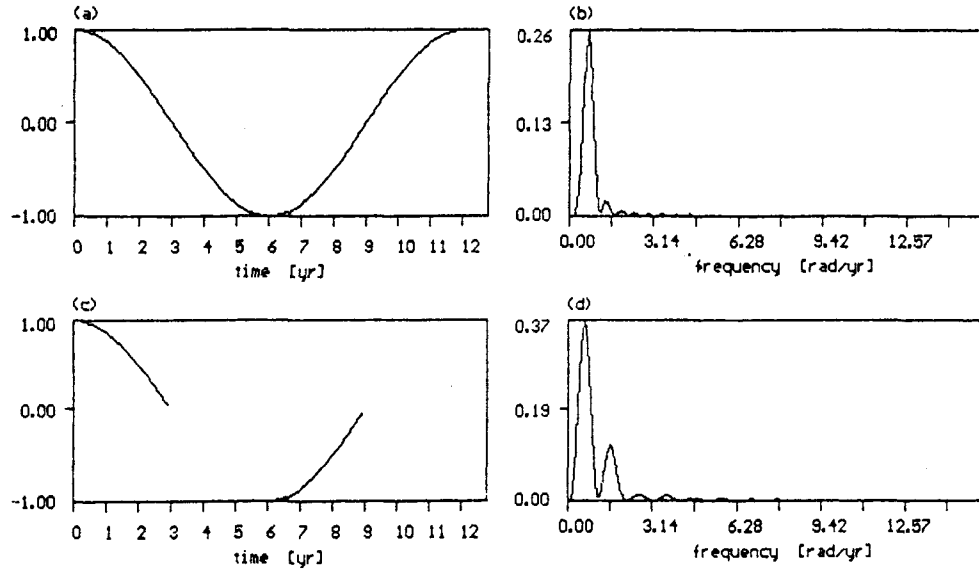


Figure 15 The largest period $P_{max} = 12$ yr, extracted from (a, b) regular observations $N = 120$; (c, d) Time Interferometer ($n_1 = 30, p = 30, n_2 = 30$).

$$P_{max}^{(N)} = N\Delta t, \quad (5.22)$$

whereas in the case of observations with a gap we have

$$P_{max}^{(b)} = 2b. \quad (5.23)$$

From Eqs. (5.20) and (5.21) we obtain again Eq. (5.3) with $\chi = 1$, from which it follows that besides the economy of observations, the Time Interferometer allows to find the period of a component, which is longer than the total time of observations (including the gap). Figure 15 confirms this result, showing that the 12 yr cosine component is registered either by 120 points of regular observations, or by 90 points of the STI, 30 points of which are missing.

5.5 The Principle of Equivalence

The comparison of the Simple Antenna and the Time Interferometer with respect to the frequency resolution, separation of lines and low frequency problem gave us Eqs. (5.3) and (5.10), which we now rewrite in the following form:

$$N = k(M + p), \quad (5.24)$$

where

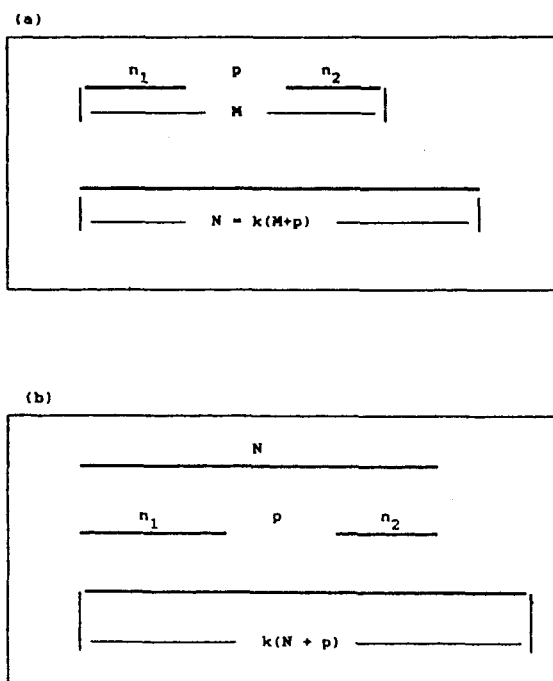


Figure 16 a, Equivalence of the Time Interferometer and the Simple Antenna with respect to the resolution frequency; b, an artificial gap improves the resolution power of the initial time series. The case $k = 1$ is illustrated.

- $k = 1$, if a complete separation of the lines and the low frequency problem is considered,
- $k = \chi$, if the resolution frequency is measured in terms of the half-power width of the spectral window's central peak,
- $\chi < k < 1$, if the partial separation of the lines is studied.

Eq. (5.24) states the *principle of equivalence*, which means that, with respect to the problems under consideration, the two-element and grating interferometers with the total amount of points M (including gaps) are equivalent to the Simple Antenna with the total amount of points $k(M + p)$ (without gaps).

Two consequences follow from the principle of equivalence. The first one implies that to achieve one and the same result (of those mentioned above), the Time Interferometer may require less time and less observations as compared with regular observations. The corresponding gains of time and observational expenditures may be estimated by Eqs. (5.4), (5.5), (5.11) and (5.12).

The second consequence leads us to a quite remarkable result: a set of regular observations, consisting of N points, has a reserve of resolution power. Indeed, it is always possible to omit p successive points (one or several times) to convert

the SA into the STI or GTI with the value χ as close to unity as possible. Such time interferometers will be equivalent to sets of regular observations consisting of $\chi(N+p)$ points. So, to improve the resolution ability of a set of regular observations, one is either to add new observations, or to omit some observed points!

The geometrical illustrations of the principle of equivalence are shown in Figure 16.

6 THE TIME INTERFEROMETER WHEN NOISE IS PRESENT

Up to now we were dealing only with deterministic functions. In this section we shall see how the Time Interferometer works when a random component of the signal is taken into account. For the sake of simplicity, we consider the time series consisting of two cosine functions and noise:

$$x_k = A_1 \cos \omega_1 t_k + A_2 \cos \omega_2 t_k + r_k, \quad k = 1, \dots, N, \quad (6.1)$$

where t_k are arbitrary set of time points, A_1, ω_1 and A_2, ω_2 are the amplitudes and frequencies of each harmonics and r_k are the normally distributed random values with zero average. The power of the noise is σ_0^2 . It is known that the power of the deterministic part in Eq. (6.1) can be defined as

$$d_0 = (A_1^2 + A_2^2)/2, \quad (6.2)$$

so the signal to noise ratio is

$$z = d_0/\sigma_0^2. \quad (6.3)$$

Since it is regarded that the time series (6.1) is comprised of the observed values x_k , the quantity σ_0 may be considered as a quantity which describes the accuracy of the instrument with respect to random errors of observations.

We are going to study how the noise changes the accuracy of the amplitude estimations, if we replace the regular observations by the equal block Time Interferometer. Usually, the frequencies ω_1 and ω_2 are obtained from the spectrum, and the amplitudes A_1 and A_2 are derived by the least squares procedure from the equation

$$\mathbf{M}\mathbf{A} = \mathbf{X}, \quad (6.4)$$

where

$$\mathbf{M} = \begin{bmatrix} (c_1, c_1) & (c_1, c_2) \\ (c_2, c_1) & (c_2, c_2) \end{bmatrix}, \quad (6.5)$$

$$\mathbf{A} = \begin{bmatrix} A_1 \\ A_2 \end{bmatrix}, \quad \mathbf{X} = \begin{bmatrix} \sum_{k=1}^N x_k \cos \omega_1 t_k \\ \sum_{k=1}^N x_k \cos \omega_2 t_k \end{bmatrix}. \quad (6.6)$$

In Eqs. (6.5)–(6.6), the following notations are used:

$$(c_i, c_i) = (N/2)[1 + P(2\omega_i)], \quad i = 1, 2, \quad (6.7)$$

$$\begin{aligned} (c_1, c_2) &= (c_2, c_1) \\ &= (N/2)[P(\omega_1 + \omega_2) + P(\omega_1 - \omega_2)], \end{aligned} \quad (6.8)$$

$$P(\omega) = \text{Re}\Omega(\omega); \quad \Omega(\omega) = \frac{1}{N} \sum_{k=1}^N \exp(-i\omega t_k). \quad (6.9)$$

The function $\Omega(\omega)$ defined by Eq. (6.9) represents a complex spectral window, satisfying the relation

$$H(\omega) = |\Omega(\omega)|^2. \quad (6.10)$$

Inverting the matrix M , we get

$$A = M^{-1}X, \quad (6.11)$$

while for the root mean square errors (r.m.s.e.) of the amplitudes we have

$$\sigma_{A_i} = s_0(m_{ii}^{-1})^{1/2}, \quad i = 1, 2, \quad (6.12)$$

where (m_{ii}^{-1}) are the diagonal elements of M^{-1} , and s_0 is an estimate of σ_0 (the r.m.s.e. of unit weight),

$$\sigma_0^2 = \frac{1}{N-2} \sum_{k=1}^N r_k^2. \quad (6.13)$$

Compare now the r.m.s.e. which we have in case of N regular observations with those which we would find for the Time Interferometer. In the former case for the function $P(\omega)$ we have

$$P(\omega) = \frac{\sin(N\omega\Delta t/2)}{N \sin(\omega\Delta t/2)}. \quad (6.14)$$

From Eqs. (6.7) and (6.8) it follows that the elements of the matrix M depend on the quantities

$$\beta_{i,j} = \begin{cases} 2\omega_i & i = 1, 2, \\ \omega_i \pm \omega_j & i, j = 1, 2, \quad i \neq j. \end{cases} \quad (6.15)$$

Suppose the $\beta_{i,j}$ are beyond the region of the central peak,

$$\beta_{i,j} > \frac{2\pi}{N\Delta t}. \quad (6.16)$$

In this case the values of $P(\beta_{i,j})$ are small since they are determined by the sidelobes of the function $P(\omega)$. Consequently, we obtain from Eqs. (6.5), (6.7) and (6.8)

$$\sigma_{A_i} = \sigma_0(2/N)^{1/2}, \quad i = 1, 2. \quad (6.17)$$

Now consider the Time Interferometer consisting of two n -point blocks of observations, separated by a p -point gap. As shown in Sect. 3, the spectral window $H(\omega)$ has sidepeaks centered at the Proper Frequencies $\bar{\omega}_k$ defined by Eq. (3.18). With respect to the sidepeaks, two situations are of interest.

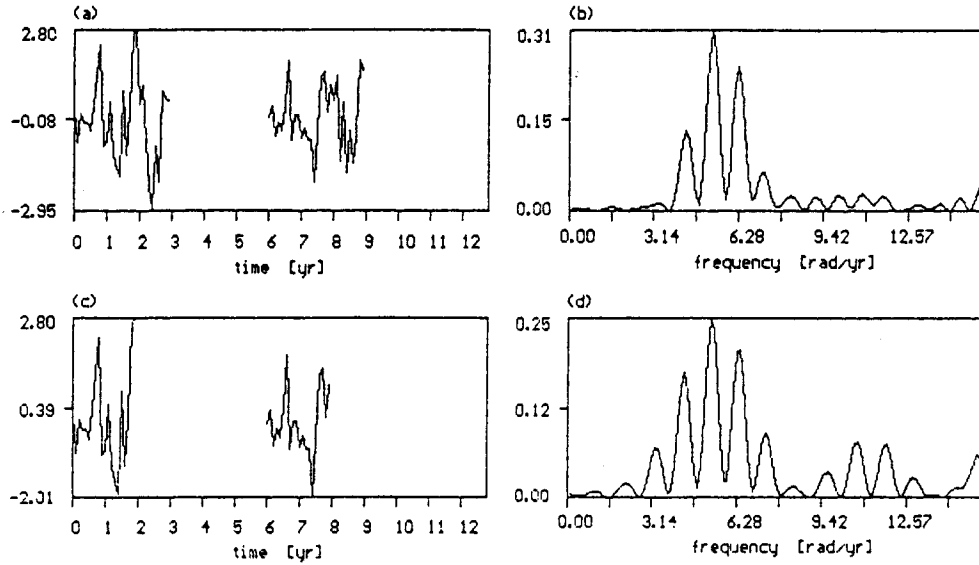


Figure 17 Spectral analysis of the same cosinusoids as in Figure 10, made by means of the Time Interferometer in the presence of noise. The signal to noise ratio is unity: a, $n_1 = 30$, $p = 30$, $n_2 = 30$; b, the resulting spectrum; c, $n_1 = 20$, $p = 40$, $n_2 = 20$; d, the resulting spectrum. Comparison is to be made with Figures 11(c, d) and 12(a, b).

1. No one of the values $\beta_{i,j}$ coincides with the Proper Frequencies (or coincides with those of PF, where the moduli of $P(\omega)$ are small). In this case it follows from Eqs. (6.6), (6.7) and (6.8)

$$\sigma_{A_i} = \sigma_0(1/n)^{1/2}, \quad i = 1, 2. \quad (6.18)$$

2. Now suppose that at least one of the $\beta_{i,j}$ happens to be a PF. Consequently, the values of $P(\beta_{i,j})$ in Eqs. (6.7) and (6.8) may be not negligibly small, and the quantities σ_{A_i} are to be calculated from the general formula (6.12). For simplicity we consider the situation when we have two close frequencies ω_1 and ω_2 such that $\omega_1 - \omega_2 = \bar{\omega}_1$. For these harmonics we have from Eq. (6.12)

$$\sigma_{A_i} = \sigma_0 n^{-1/2} [1 - H(\bar{\omega}_1)]^{-1/2}, \quad i = 1, 2. \quad (6.19)$$

From Eqs. (6.17)–(6.19), it follows that the transition from regular observations to the Time Interferometer results in larger errors of the amplitude (if in both cases the accuracy σ_0 of the instrument remains the same). Thus, to obtain the same reliability, the Time Interferometer is to treat the more accurate observations. Still, if the observations are of good accuracy, it may happen that the Time Interferometer will produce quite reliable results. As an example, we consider the time series of latitude variations, consisting of the so-called normal points, following each other over 0.1 year. This time series is known to be generated by the annual and Chandler's ($P \sim 1.2$ yr) waves, and the accuracy of each point is evaluated to be $\sigma_0 = 0.2''$.

To resolve the two lines completely, one needs $N = 120$ regularly spaced points, so from Eq. (6.17) we have

$$\sigma_{A_i} = 0.02''/\sqrt{60}. \quad (6.20)$$

At the same time, for the Time Interferometer with $n = 10$, $p = 50$ (and it is the most extreme case, since $H(\omega_1 - \omega_2) = 0.9$) we find from Eq. (6.19)

$$\sigma_{A_i} = 0.02''. \quad (6.21)$$

Taking into consideration that the amplitudes of the annual and of Chandler's components are of order $0.1''$, we see that even in the most unfavourable case the root mean square errors satisfy the rule of three sigmas.

Still one question remains: what the upper limit of noise is permissible to derive statistically reliable amplitudes and to have at the same time spectral lines at frequencies ω_1 and ω_2 still recognizable? Guided by the rule of three sigmas, one has from Eq. (6.12)

$$3\sigma_0(m_{ii}^{-1})^{1/2} = A_i, \quad i = 1, 2. \quad (6.22)$$

Now, we find from Eq. (6.3)

$$z = 9d_0 m_{ii}^{-1}/A_i^2, \quad i = 1, 2. \quad (6.23)$$

Figure 17 shows the Time Interferometer with $n = 30$, $p = 30$; $n = 20$, $p = 40$, generated for the functions (5.14). The noise level was chosen in such a way that the signal to noise ratio, $z = 1$, does not exceed the critical value defined by Eq. (6.23). Nevertheless, as one can see, the true peaks are well recognizable.

7 THE OPTIMIZATION OF THE TIME INTERFEROMETER

As we have seen in Sect. 5, the beneficial properties of the equal block Time Interferometer over the regular observations depend on p/n . The longer the gap, the better the interferometer works. On the other hand, very long baseline Time Interferometer ($p \gg n$) produces a spectral window which contains so many sidepeaks that the resulting spectrum becomes hardly understandable. Moreover (see Sect. 6), a small number of observations and large values of p/n deteriorate the reliability of the amplitude determination. In practice, optimal ratios p/n are to be taken in order to meet these contradictory requirements. Numerous numerical tests give confidence that if the Time Interferometer with equal blocks of observations is used, the optimal values are $p/n = 1 \div 2$. In this case when the baseline b satisfies (5.19), a complete separation of close harmonics is possible, and the first sidepeak is not too large to confuse the interpretation of the spectrum. The Time Interferometer with unequal blocks is more preferable in some cases since it suppresses, to some extent, the sidepeaks though does not resolve two close lines completely. The recommended ratios for the parameters n_1 , p and n_2 are: $n_1 = p$, $n_2 \leq n_1/2$.

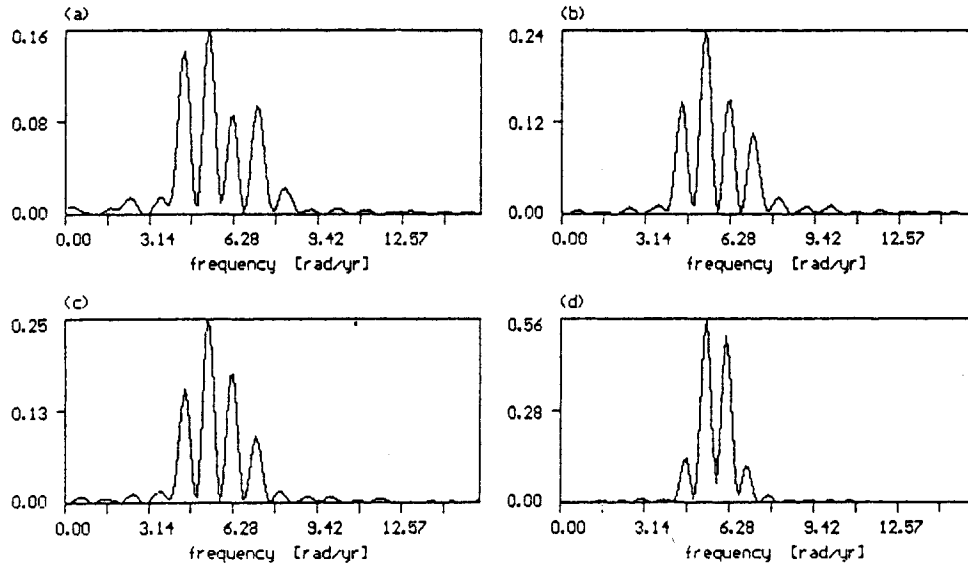


Figure 18 Separation of the annual and Chandler's components in spectra of the PVL by means of the equal block Time Interferometers: a, $n_1 = 32, p = 32, n_2 = 32$; b, $n_1 = 33, p = 33, n_2 = 33$; c, $n_1 = 34, p = 34, n_2 = 34$; d, $n_1 = 40, p = 40, n_2 = 40$; b = 6.4 yr, $L = 9.5$ yr; b, $n_1 = 33, p = 33, n_2 = 33$; b = 6.6 yr, $L = 9.8$ yr; c, $n_1 = 34, p = 34, n_2 = 34$; b = 6.8 yr, $L = 10.1$ yr; d, $n_1 = 40, p = 40, n_2 = 40$; b = 8.0 yr, $L = 11.9$ yr.

8 APPLICATIONS OF THE TIME INTERFEROMETER TO ASTROMETRIC OBSERVATIONS

To show how the Time Interferometer works when data are taken from observations, we chose a time series of the polar variations of the latitude (henceforth, PVL),

$$\Delta\phi(t) = x(t) \cos \lambda - y(t) \sin \lambda, \quad (8.1)$$

where the coordinates of the pole $x(t), y(t)$ were taken from the Annual Reports of BIH for 1967 to 1986 at the interval $\Delta t = 0.1$ yr. The values $\Delta\phi(t)$ correspond to longitude λ of the Pulkovo Observatory. In Sect. 6 we have only mentioned the PVL, now we are going to use it in order to see how the Time Interferometer separates the annual and Chandler's harmonics.

All the properties of the Time Interferometer described in previous sections may be fully realized only if we know *a priori* the frequencies of the harmonics. In most practical cases, either no *a priori* information is available, or the information is not complete. Keeping this in mind, we treated the PVL by various methods, each time making different assumptions on what kind of *a priori* information is suggested.

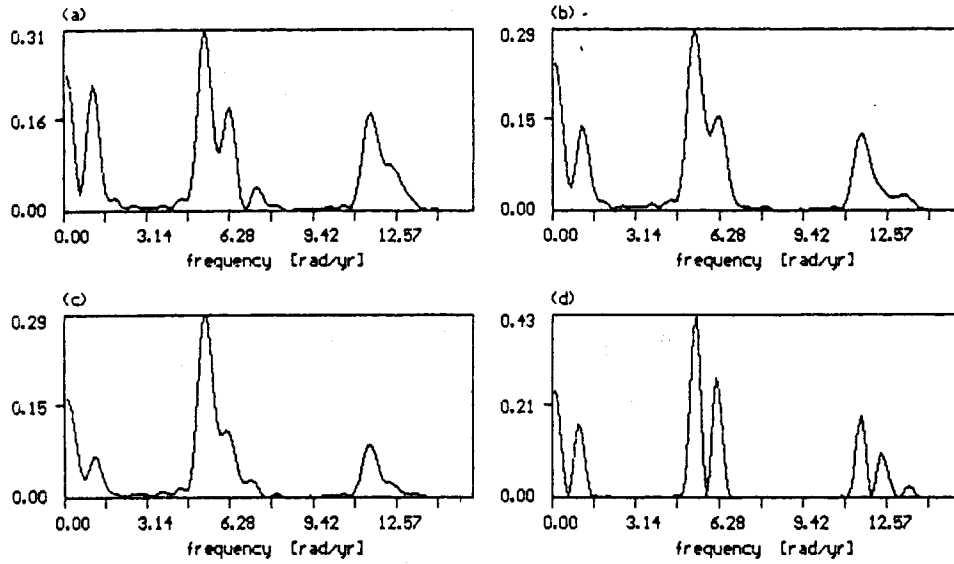


Figure 19 Separation of the annual and Chandler's components in spectra of PVL by means of the Grating Time Interferometers: a, $n = 4$, $p = 6$, $m = 10$; $L = 9.5$ yr; b, $n = 5$, $p = 5$, $m = 10$; $L = 9.4$ yr; c, $n = 6$, $p = 4$, $m = 10$; $L = 9.3$ yr; d, $n = 5$, $p = 5$, $m = 14$; $L = 13.4$ yr.

8.1 Regular Observations

Power spectra of the PVL calculated for successively increasing number of observations show that the annual and Chandler's lines are not separated until 90 points are available; the complete separation is provided by 133 points. The estimations of the periods made by means of the parabolic interpolation over three adjacent spectral readings yield: $P_1 = 1.00$ and $P_2 = 1.18$ yr.

8.2 The Time Interferometer with Equal Blocks. Complete Information is Available

Suppose we know exactly the periods of the harmonics to be separated ($P_1 = 1.00$ and $P_2 = 1.18$ yr). In this case, from Eq. (5.19) we find that the baseline of a suitable interferometer is equal to 6.67 yr, hence we may take $n = p = 33$ or 34 to separate the two lines completely (Figure 18b, c).

8.3 The Time Interferometer with Equal Blocks. Approximate Information is Available

Let us assume that we are not sure that the periods we know are exact, but we admit that errors do not exceed 30 per cent. Thus we may adopt $n = p = 32$ or 40.

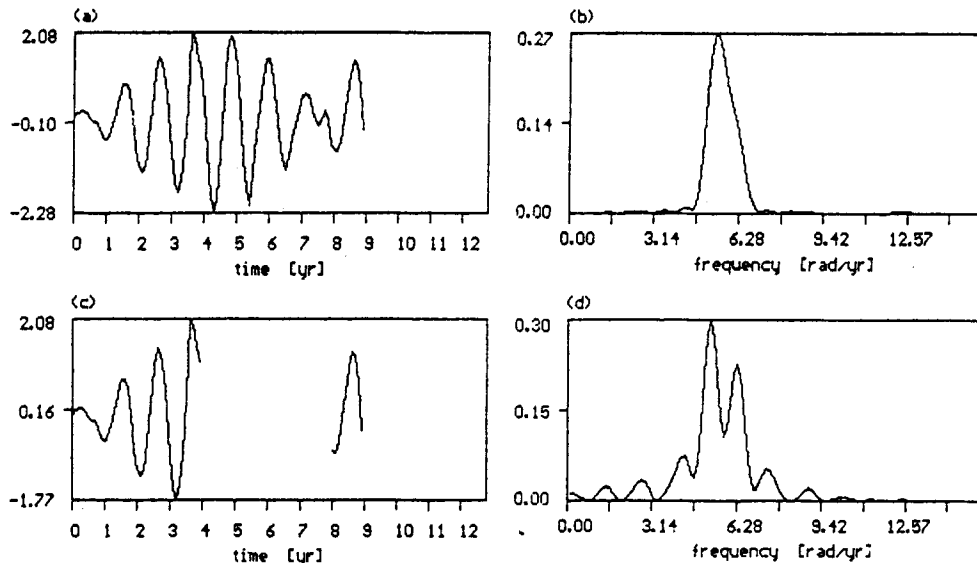


Figure 20 Separation of the annual and Chandler's components in spectra of the PVL by means of an artificial gap: *a*, regular observations, $N = 90$, $\Delta\phi(t)$ in 0.01 of arcsec; *b*, no separation is visible in the spectrum; *c*, the artificial gap produced the Time Interferometer $n_1 = 40$, $p = 40$, $n_2 = 10$; $b = 6.5$ yr, $M = 90$; *d*, separation of the lines is clearly visible in the spectrum, $C = 0.45$.

Figures 18(a), 18(d) show that the Time Interferometer is able to show the double structure with a good separation.

8.4 The Grating Interferometer.

Approximate Information is Available

Suppose that we do not know the periods exactly but we are sure that the double line is situated somewhere in the vicinity of the frequency $\omega = 2\pi$ rd/yr. In this case we may try regular observations with periodic gaps (the Grating Time Interferometer). As can be seen from Figure 4, the sidepeaks of the spectral window are far from the central peak. For this reason (Figure 19) the spectrum contains several replicas of our double line, but the knowledge of approximate periods enables us to find the correct replica in the spectrum. We see that a partial resolution is available at the time spans $L = 9.3 \div 9.5$ yr, and a full separation is attained at $L = 13.4$ yr. In this case we save not time, but labour expenditure up to 40 ÷ 60 per cent.

8.5 The Time Interferometer with Unequal Blocks.

No a Priori Information is Available

In this case it seems that the interferometric idea is hopeless. But recalling that a set of regular observations has always a reserve of the resolution power, we may

combine the regular observations with the abilities of the Time Interferometer. Making successive acquisition of data, we have found that when the total amount of points reached $N = 90$, the broad line in the spectrum of PVL lost its symmetrical form giving suspicion of duplicity (see Figure 20b). In accordance with the property of the artificial gap, stated in Sect. 5, we may omit some points in order to make the rest of them to be equivalent to a more extended time series. Keeping in mind that a non-equal block Time Interferometer suppresses the sidepeaks, we may place step by step the gap inside the time series in such a way that, for every value of increasing parameter n_2 , other parameters are taken as

$$n_1 = p = (N - n_2)/2, \quad (8.2)$$

where $N = \text{const}$ (in our example, $N = 90$). Figure 20 demonstrates the result, obtained with the help of an artificial gap, which produced the Time Interferometer $n_1 = 40$, $p = 40$, $n_2 = 10$, $b = 6.5 \text{ yr}$, $M = 90$. The comparison of Figures 20(b) and 20(d) shows how the gap helped us to see clearly the two lines without additional observations.

9 CONCLUSIONS

Usually, all advantages are to be paid for. In our case, the surprising abilities of the Time Interferometer are paid by the contamination of the spectrum. The longer the gaps the better close harmonics are separated, the more dirty the spectrum becomes. To extract the true information from the contaminated spectra, we should have either sufficient a priori information of the process under consideration (and it is the predominant idea of the present work), or to use a suitable restoration technique (and it is a topic for a further study). The main goal of this work was to show that gaps in observational series are not to be afraid of, moreover, in some applications they may be used to improve the resolution abilities of power spectra, provided that the time series is stationary and nothing drastic is expected inside the gaps. The concept of the Time Interferometer, introduced in this paper, is very instructive, for it helps us to understand many unusual properties of time series with gaps from the standpoint of radio astronomy, where the corresponding properties of interferometers are usual.

The author appreciates the support of this work by a grant of the American Astronomical Society.

References

- Deeming, T. J. (1975a) *Astrophys. Space Sci.* **36**, 137.
 Deeming, T. J. (1975b). *Astrophys. Space Sci.* **42**, 257 (E).
 Delache, P. and Scherer, P. H. (1983) *Nature* **306**, 651.
 Duvall, T. L., Jr. and Harvey, J. W. (1984) *Nature* **310**, 19.
 Jenkins, G. M. and Watts, D. G. (1968) *Spectral Analysis and Its Applications* Holden-Day, San Francisco.

- Marple, Jr., S. L. (1987) *Digital Spectral Analysis with Applications* Prentice-Hall, Englewood Cliffs, New Jersey.
- Otnes, R. K. and Enochson, L. (1978) *Applied Time Series Analysis* A Wiley-Interscience Publication, New York.
- Roberts, D. H., Lehar, J., and Dreher, J. W. (1987). *Astron. J.* **93**, 968.